ORIGINAL ARTICLE



Effects of Sacral Slope Changes on the Intervertebral Disc and Hip Joint: A Finite Element Analysis

Yogesh Kumaran¹, Norihiro Nishida², Sudharshan Tripathi¹, Muzammil Mumtaz¹, Takashi Sakai², Hossein Elgafy¹, Vijay K. Goel¹

- OBJECTIVE: Spinopelvic parameters are vital components that must be considered when treating patients with spinal disease. Several finite element (FE) studies have explored spinopelvic parameters such as sacral slope (SS) and the impact on the lumbar spine, although no study has examined the effect on the hip and sacroiliac joint (SIJ) on varying SS angles. Therefore, it is necessary to have a biomechanical understanding of the impact on the spinopelvic complex.
- METHODS: An FE lumbar, pelvis, and femur model was created from computed tomography scans of a 55-year-old female patient with no abnormalities. Three models were created: a normal model (SS = 26°), a model with high SS (SS = 30°), and a model with low SS (SS = 20°). These models underwent loading for flexion, extension, lateral bending, and axial rotation. Range of motion (ROM), intradiscal pressures, hip joint, and SIJ contact stresses were analyzed.
- RESULTS: The high SS model (SS = 30°) indicated the highest ROM in the L5-S1 (slip angle) level and the highest intradiscal pressures. The highest average hip and SIJ contact stresses were present in this model, although the low SS model (SS = 20°) in extension had the largest stresses for the hip and SIJ.

■ CONCLUSIONS: The results provide evidence that patients with higher SS may be more prone to increased ROM at the slip angle (L5-S1). In addition, patients with higher SS were shown to have higher contact stresses on the hip joint and SIJ, potentially leading to SIJ dysfunction. Clinically, correcting lumbar lordosis including SS is important; however, a high SS may have a negative impact on the intervertebral disc, SIJ, and hip joint.

INTRODUCTION

he spine, pelvis, and hip comprise a complex system that is required for the maintenance of sagittal balance of the spine. Lumbar lordosis (LL), pelvic incidence (PI), pelvic tilt (PT), and sacral slope (SS) are key spinopelvic parameters that alter one another. LL is defined as the angle between the first and fifth lumbar vertebrae superior end plates [2]. PI is defined as the angle between the line perpendicular to the midpoint of the sacral end plate and a line connecting this point to the midpoint of the axis of the femoral head [3]. PT is the angle between the line connecting the midpoint of the superior sacral plate to the center axis of the femoral heads and a vertical reference line from the femoral head. SS is the angle between the superior sacral end plate and a horizontal reference line. The PI is correlated to the SS and

Key words

- Finite element analysis
- Hip joint
- Pelvic tilt (PT)
- Sacral slope (SS)
- Sacroiliac joint (SIJ)

Abbreviations and Acronyms

FE: Finite element IVD: Intervertebral disc LL: Lumbar lordosis PI: Pelvic incidence

PLIF: Posterior lumbar interbody fusion

PLF: Posterolateral fusion

PT: Pelvic tilt

ROM: Range of motion SIJ: Sacroiliac joint

SS: Sacral slope

SSD: Decreased sacral slope model SSI: Increased sacral slope model

From the ¹Engineering Center for Orthopedic Research (E-CORE), Departments of Bioengineering and Orthopedic Surgery, University of Toledo, Toledo, Ohio, USA; ²Department of Orthopedic Surgery, Yamaguchi University Graduate School of Medicine, Ube City, Yamaguchi Prefecture, Japan

To whom correspondence should be addressed: Vijay K. Goel, Ph.D.

[E-mail: Vijay.Goel@utoledo.edu]

Citation: World Neurosurg. (2023) 176:e32-e39. https://doi.org/10.1016/j.wneu.2023.03.057

Journal homepage: www.journals.elsevier.com/world-neurosurgery

Available online: www.sciencedirect.com

1878-8750/\$ - see front matter © 2023 Elsevier Inc. All rights reserved.

LL, where the PI is the algebraic sum of the SS and PT angles (PI = PT + SS) [3, 39, 40].

Changes in SS secondary to reduction of LL affect the biomechanics of the lumbar spine and result in deterioration of sagittal balance. In addition, these changes to the sagittal balance have been known to play a role in various diseases, including disc degeneration and low back pain. Recently, there have been numerous reports of the importance of the sagittal spinopelvic alignment in isthmic spondylolisthesis and increased SS. An increased slip angle, which is defined as the angle between the L5 and S1 end plates, and a vertical orientation of the L5-S1 intervertebral disc (IVD) are also associated with progression of spondylolisthesis.

The spinopelvic complex compensates for the sagittal imbalance of the spine through pelvic retroversion with a decreasing SS.⁹ When the lumbar spine endures IVD degeneration or other spinal diseases, it becomes more kyphotic, changing the spinopelvic parameters. One area that remains unexplored is the effect of the SS on the sacroiliac joint (SIJ) and hip joint. It is vital for clinicians to understand how these spinopelvic parameters such as SS influence the biomechanics of various components, including the SIJ, hip joint, and IVDs.

We hypothesize that a finite element (FE) lumbar spinopelvic model with varying SS angles and multiple motions may alter the biomechanics of the IVD, SIJ, and hip joints. There are several FE analyses examining changes in SS, although these models typically consider only the lumbar spine and sacrum. To our best knowledge, there are no studies that have analyzed the mechanics of the SIJ, hip joint, and IVD in varying SS angles. The current study used a three-dimensional FE female lumbar spine-pelvic-femur model to examine how stress and mobility in the model changed for various SS angles.

METHODS

FE Model of Lumbar Spine Pelvis

A previously developed and validated FE lumbar spine, pelvis, and femur model¹² was used for this study (Figures 1 and 2). The geometry of the model was generated from computed tomography of a 55-year-old female patient without any abnormalities, degeneration, or deformation in bony features. The relevant approvals were obtained for the use of these images at the corresponding author's facility. Three-dimensional geometry of the lumbar spine pelvis model was built from MIMICS software (Materialise, Leuven, Belgium). For geometry smoothing, Geomagic Studio software (Raindrop Geomagic Inc., Raleigh, North Carolina, USA) was used. After the geometry was smoothed, the intervertebral discs were meshed using IAFEMESH (University of Iowa, Iowa City, Iowa, USA), whereas the vertebrae and pelvis were meshed using Hypermesh (Altair Engineering Inc., Troy, Michigan, USA). The thickness of cortical bone for the vertebrae and pelvis was 1 mm surrounding the cancellous bone. After the FE model geometry was developed, all meshed regions were assembled in Abaqus FEA software (Dassault Systèmes/Simulia Inc., Providence, Rhode Island, USA). The cortical bone of the vertebrae and intervertebral discs was assigned with linear hexahedral elements, whereas the cancellous bone of both vertebrae and pelvis was assigned with tetrahedral elements.

Truss elements were used for the ligamentous tissues which included the anterior longitudinal ligament, posterior longitudinal ligament, interspinous ligament, supraspinous ligament, capsular ligament, and ligamentum flavum in the lumbar spine. The model also includes the anterior sacroiliac ligament, interosseous ligament, long posterior sacroiliac ligament, short posterior sacroiliac

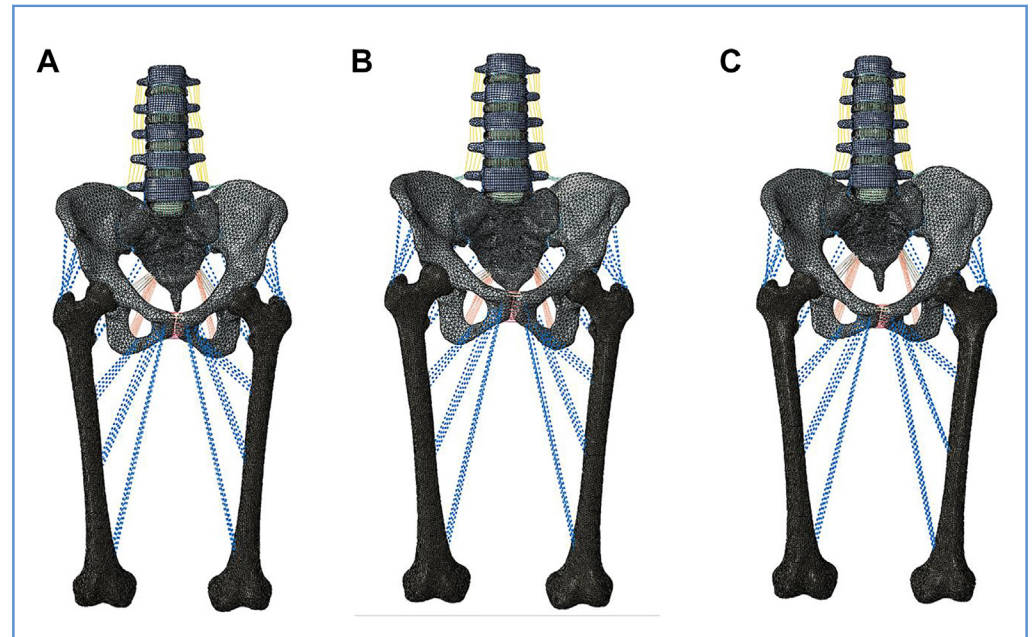
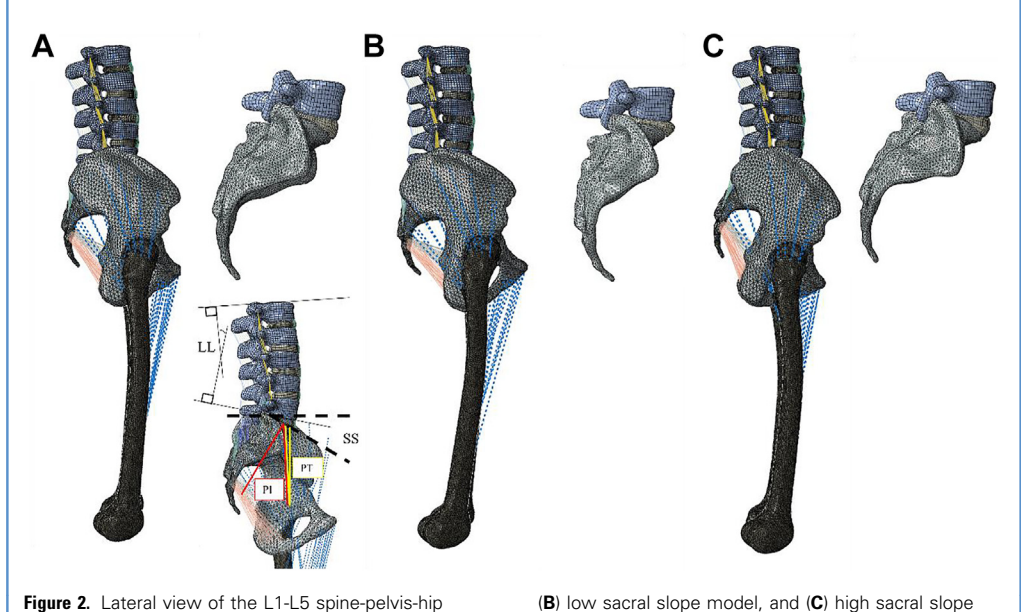


Figure 1. Front view of the L1-L5 spine-pelvis-hip finite element model. (A) Intact model, (B) low sacral slope model, and (C) high sacral slope model.



finite element model. (A) Intact model showing sacral slope, lumbar lordosis, pelvic incidence, and pelvic tilt,

ligament, sacrospinous ligament, and sacrotuberous ligament. The SIJs, spine facets, articular cartilages, and pubic symphysis were modeled with nonlinear soft contacts.

The femur was positioned relative to the pelvis per Wu et al.¹³ by first defining the anatomic planes of each femur based on femoral bony features and the hip joint center of rotation and then aligning these defined planes with the anatomic planes of the pelvis. Hip joint functionality was validated against research conducted by Anderson et al. 14,15 and Harris et al. 14,15 The experimental study simulated motions, specifically walking, ascending stairs, and descending stairs,14 described in an earlier instrumented hip clinical study by Bergmann et al.16 This study validated hip functionality by comparing hip contact stress and area against those determined by Anderson et al. 14,15 (described earlier) and Harris et al. 14,15 Harris et al. 15,16 developed patient-specific FE models based on volunteers' scans, but the relative positions of the femoral heads and acetabula of these models were driven per data from Bergmann et al. 15,16; contact metrics produced by the models were measured and reported. The same boundary conditions and activities were simulated in the current work: the pelvis was constrained while the femur was positioned per the Bergmann et al. 16 angles corresponding to walking, ascending stairs, and descending stairs. This normal spine-pelvis-hip model was considered as the intact model. The spinopelvic parameters of this model were SS = 26° , LL = 42° , PI = 37° , and PT = 11° , respectively (Figures 1A and 2A). The intact model was assembled in Abaqus 6.14, and the final model contained 767,694 elements.

Material Properties

The material properties of the structures in the FE model for cortical and cancellous bones, annulus fibrosa, nucleus pulposa, ligaments, and joints are summarized in Table 1.23-27 Muscles spanning the hip joint from their physiologic origins to insertions were included as connector elements with stiffnesses assigned per Phillips et al. 19,28,29 (Table 1). 19,28,29 These muscles included the gluteus maximus, medius, and minimus, adductor longus, magnus and brevis, and the psoas major.

Models with Various SS Degrees

To investigate the biomechanical influence of SS, the intact model was modified with various SS degrees (20° and 32°, respectively) by rotating the sacrum and pelvis.2 These models were considered as the low SS model (SSD) and the high SS model (SSI), respectively. The spinopelvic parameters for the SSD model were SS = 20° , LL = 36° , PI = 37° , and PT = 17° , respectively (Figures 1B and 2B). The parameters for the SSI model were SS = 32° , LL = 42° , PI = 37° , and PT = 5° , respectively (Figures 1C and 2C). The angles described fell within the range of a radiologic study performed by Os et al.2

Loading and Boundary Conditions

A 400 N compressive follower load was applied tangentially to each vertebra of the spine using wire elements to simulate the effect of muscle forces and the weight of the upper trunk. 12 A pure moment of 7.5 Nm was applied to the superior surface of L1 to simulate the physiologic motions of flexion, extension, left and right lateral bending, and left and right axial rotation. To constrain the models, the femurs were fixed in all degrees of freedom to prevent relative displacement of the legs in 2-leg stance condition. 26,27

Component	Material Properties	Constitutive Relation	Element Type
oomponent	material riopetites	neiduui	Figurent Type
Vertebral cortical bone ¹⁷	E = 12,000 MPa	Isotropic, elastic	8 nodes brick element (C3D8)
	$\upsilon = 0.3$		
Vertebral cancellous bone ¹⁷	E = 100 MPa	Isotropic, elastic	4 nodes tetrahedral element (C3D4)
	v = 0.2		
Pelvic cortical bone (sacrum, ilium) ¹⁴	E = 17,000 MPa	Isotropic, elastic	4 nodes tetrahedral element (C3D4
	$\upsilon = 0.3$		
Sacrum cancellous bone ¹⁸	Heterogeneous	Isotropic, elastic	4 nodes tetrahedral element (C3D4
llium cancellous bone ¹⁸	<i>E</i> = 70 MPa	Isotropic, elastic	4 nodes tetrahedral element (C3D4
	v = 0.2		
Femur cortical bone ¹⁹	<i>E</i> = 17,000 MPa	Isotropic, elastic	4 nodes tetrahedral element (C3D4
	v = 0.29		
Femur cancellous bone ¹⁹	E = 100 MPa	Isotropic, elastic	4 nodes tetrahedral element (C3D4)
	v = 0.2		
Ground substance	$C_{10} = 0.035$	Hyperelastic anisotropic (HGO)	8 nodes brick element (C3D8
of annulus fibrosis ²⁰	$K_1 = 0.296$		
	$K_2 = 65$		
Nucleus pulposus ¹⁷	<i>E</i> = 1 MPa	Isotropic, elastic	8 nodes brick element (C3D8
	v = 0.499		
Anterior longitudinal ¹⁷	7.8 MPa (<12%), 20 MPa (>12%)	Nonlinear hypoelastic	Truss element (T3D2)
Posterior longitudinal ¹⁷	10 MPa (<11%), 20 MPa (>11%)	Nonlinear hypoelastic	Truss element
Ligamentum	15 MPa (<6.2%), 19.5	Nonlinear	Truss element
flavum ¹⁷	MPa (>6.2%)	hypoelastic	(T3D2)
Intertransverse ¹⁷	10 MPa (<18%), 58.7 MPa (>18%)	Nonlinear hypoelastic	Truss element (T3D2)
Interspinous ¹⁷	10 MPa (<14%), 11.6 MPa (>14%)	Nonlinear hypoelastic	Truss element (T3D2)
Supraspinous ¹⁷	8 MPa (<20%), 15 MPa (>20%)	Nonlinear hypoelastic	Truss element (T3D2)
Capsular ¹⁷	7.5 MPa (<25%), 32.9 MPa (>25%)	Nonlinear hypoelastic	Truss element (T3D2)
Anterior sacroiliac joint ²¹	125 MPa (5%), 325 MPa (>10%), 316 MPa (>15%)	Nonlinear hypoelastic	Truss element (T3D2)
Short posterior SI ²¹	43 MPa (5%), 113 MPa (>10%), 110 MPa (>15%)	Nonlinear hypoelastic	Truss element (T3D2)

Table 1. Continued				
Component	Material Properties	Constitutive Relation	Element Type	
Long posterior SI ²¹	150 MPa (5%), 391 MPa (>10%), 381 MPa (>15%)	Nonlinear hypoelastic	Truss element (T3D2)	
Intraosseus ²¹	40 MPa (5%), 105 MPa (>10%), 102 MPa (>15%)	Nonlinear hypoelastic	Truss element (T3D2)	
Sacrospinous ²¹	304 MPa (5%), 792 MPa (>10%), 771 MPa (>15%)	Nonlinear hypoelastic	Truss element (T3D2)	
Sacrotuberous ²¹	326 MPa (5%), 848 MPa (>10%), 826 MPa (>15%)	Nonlinear hypoelastic	Truss element (T3D2)	
Gluteus maximus ²²	k = 344 N/mm	_	Connector element	
Gluteus medius ²²	k = 779 N/mm	_	Connector element	
Gluteus minimus ²²	k = 660 N/mm	_	Connector element	
Psoas major ²²	k = 100 N/mm	_	Connector element	
Adductor magnus ²²	k = 257 N/mm	_	Connector element	
Adductor longus ²²	k = 134 N/mm	_	Connector element	
Adductor brevis ²²	k = 499 N/mm	_	Connector element	

DATA ANALYSIS

After the generation of each model, an FE analysis of the models was performed in Abaqus 2019 (Dassault Systems). The range of motion (ROM), intradiscal (nucleus) stresses, left-right average hip contact stress (MPa), and left-right average SIJ contact stress (MPa) were calculated for the intact, SSD, and SSI models. The maximum von Mises stress was noted for the nucleus stresses.

The percentage change (%) was calculated using the following equation:

$$\label{eq:percentage} Percentage \, change \, (\%) = \frac{\text{SSD} \, (\text{SSI}) \, \text{model data} - \text{intact model data}}{\text{Intact model data}} \times \text{100}$$

RESULTS

ROM

The study indicated that the ROM for all motions in SSI increased compared with the intact model at L5-S1 and the overall L1-S1 ROM (Figure 3A and B). Marginal differences were seen at other lumbar levels in both SSD and SSI (L1-L5) and were not plotted graphically. In extension, the ROM of the SSD and SSI models at both L5-S1 and L1-S1 was higher compared to the intact model (4% and 22%).

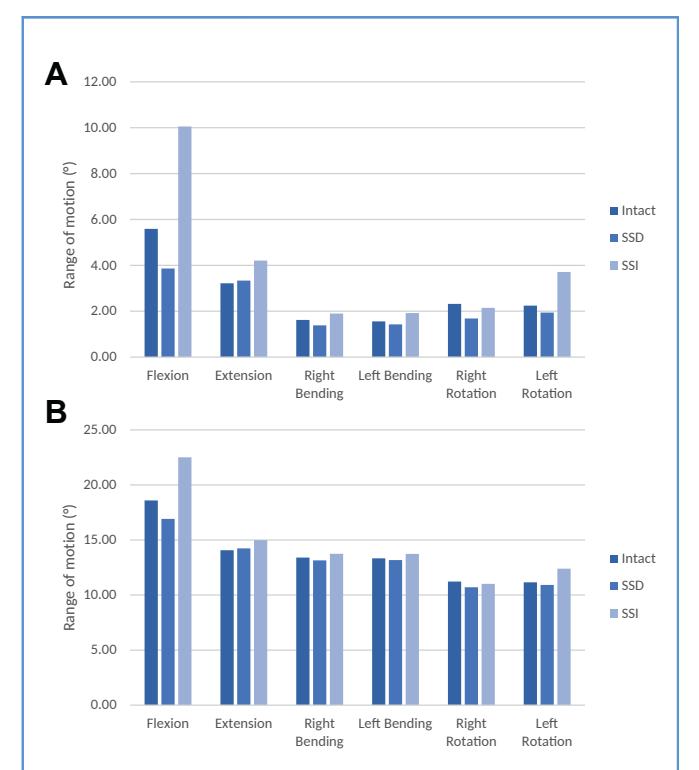


Figure 3. Range of motion of L5-S1 (**A**) and overall range of motion (**B**) (L1-S). The *vertical axis* shows the angle (°) and the *horizontal axis* shows the motions simulated. SSD, low sacral slope model; SSI, high sacral slope model.

increase at L5-S1 and 1% and 6% increase at L1-S1 compared to the intact model, respectively). The largest changes were seen in flexion as the ROM of the SSD models showed a decrease at L5-S1 and L1-S1 compared to the intact model (31% at L5-S1 and 9% at L1-S1, respectively). The ROM of the SSI models for flexion increased by 80% at L5-S1 and 21% at L1-S1 compared to the intact model, respectively. Marginal changes were seen in lateral bending for the ROM of both the SSD and SSI models. Rotation showed increased ROM for SSI, specifically in left rotation, whereas the SSD case showed marginal decreases compared with the intact model.

Maximum Intradiscal Pressures

Maximum intradiscal pressures indicated large increases at the lumbosacral junction (L5-S1) with marginal increases and decreases at other lumbar levels (L1-L5) (Figure 4). The largest percent increase was seen in right bending for the SSI model, which showed a 145% increase compared with the intact model. Lateral bending indicated the highest intradiscal pressure of 4.4 MPa in the SSI model, indicating that this motion was affected most by the high SS.

Left-Right Average Hip Joint Contact Stress

Average hip joint contact stresses of the left and right femoral heads was recorded for all models (Figure 5). Both SSD and SSI showed higher hip joint contact stresses compared with the intact model for all motions. SSI indicated higher contact

stresses for all motions, except for extension. Extension showed a slightly larger increase in hip joint contact stress for SSD compared with the SSI model (increase of 11% for SSD and 8% for SSI, respectively, compared with the intact model). The largest contact stress was seen in flexion for the SSI model, which indicated a 38% increase compared with the intact model.

Left-Right Average SIJ Contact Stress

Average SIJ contact stresses of the left and right SIJ interfaces were recorded and averaged for both surfaces (Figure 6). The study indicated that SIJ stresses for the SSI model showed increases in all motions compared with the intact model except for extension, which showed a 19% decrease. The SSD model SIJ stresses indicated an increase of 8% compared with the intact model for extension. A marginal increase was seen in right rotation for the SSI model compared with the intact model. For all the other motions, a low SS indicated decreased SIJ stress compared with the intact model, whereas high SS indicated higher SIJ stresses compared with the intact model. For the SSI model, flexion showed the largest increase in SIJ stress of 25% compared with the intact model.

DISCUSSION

The objective in this study was to investigate the biomechanical characteristics after changes in sagittal spinopelvic parameters, specifically with changes to the SS. Adult spinal deformity continues to be a disabling condition for patients worldwide. Therefore, elucidating how spinopelvic parameters contribute to spine and hip conditions is important for clinicians. In this study, we used a previously validated female FE model to analyze the effect of changes in the SS angle on ROM and stresses of the spine and pelvis.

Several previous studies have performed biomechanical analyses to examine changes in the SS and its effect on instrumentation. In a fresh-frozen cadaver study of the spine from L5 to S1 examining anterior lumbar interbody fusion, Drazin et al. $^{3^{\circ}}$ loaded specimens under compression at a $20^{\circ}-50^{\circ}$ SS angle with increments of 10° .

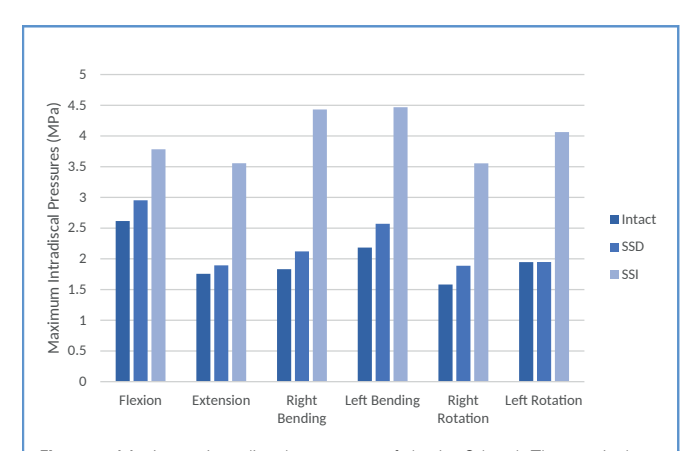


Figure 4. Maximum intradiscal pressures of the L5-S level. The *vertical axis* shows stress (MPa) and the *horizontal axis* shows the motions simulated. SSD, low sacral slope model; SSI, high sacral slope model.

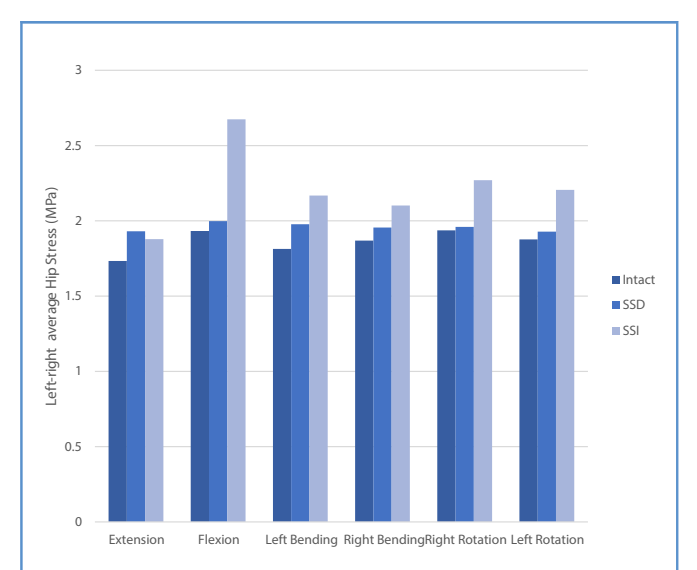


Figure 5. Left-right average hip joint contact stresses for all motions. The *vertical axis* shows stress (MPa) and the *horizontal axis* shows the motions simulated. SSD, low sacral slope model; SSI, high sacral slope model.

These investigators found that a high SS angle induced a decrease in axial stiffness resulting from the increase of SS, especially >30°. Chen et al. performed an FE analysis on posterolateral fusions (PLF) and posterior lumbar interbody fusion (PLIF) with SS angles of 35°-55°. These investigators identified that patients with high SS angles who have isthmic spondylolisthesis may be better candidates for PLIF rather than PLF because of the high stresses seen on PLF instrumentation. These studies confirmed that increased SS negatively affects surgical instrumentation, increasing the stress on the sacral screws in PLF and PLIF models. However, because corrections are usually made in 10° increments, it was believed necessary to analyze the effects of more minor angular changes, therefore, in the present intact model with a SS of 26° and was varied by 6°. Previous reports in the literature analyzed only the lumbar spine; however, the current study examines the pelvis and hip joint.

The results of the current study are consistent with previous studies examining total lumbar ROM (L1-S) that indicated increases as the SS increased, 10 except for right rotation, which indicated a slight decrease compared with the intact model. As the SS increased, the L5-S1 (slip angle) ROM increased for all motions, other than extension, which showed negligible change in ROM. In the decreased SS case, the ROM decreased at L5-S1 compared with the intact model. It is evident from the results that patients with higher SS and slip angles may be more prone to develop isthmic spondylolisthesis compared with patients with decreased SS, which is consistent with several clinical studies. For example, Vialle et al.⁷ reported significantly higher PI and SS values in patients with isthmic spondylolisthesis compared with controls. Oh et al.³¹ observed that PI and SS were significantly higher in a group of young males with spondylolysis (and low-grade spondylolisthesis) compared with an age-matched and sex-matched control group of individuals without spondylolysis.

Furthermore, the data regarding stresses on IVDs for all motions indicated increased stresses on the L5-S IVD in both the patients with low SS and the patients with high SS, although the largest increase in IVD stress was seen in the patient with high SS compared with a patient with a normal SS. This finding can be explained by the increased SS and decreased PT in the SSI model causing increased posterior compression and shift of the shearing force line on the IVD.9 The model with low SS also showed an increase in L5-S IVD compared with the intact model. In addition, the increased ROM at L5-S1 indicates slipping of the intervertebral level, leading to increased stress on the posterior portion of the IVD. A clinical study by Roussouly et al. 17 proposed the "nutcracker" (low PI and low SS) and "shear-type" (high PI and high SS) mechanisms for the development of defects on the lumbosacral junction in patients with abnormal spinopelvic parameters. These investigators discussed that a more vertical orientation of the sacral end plate led to the increased shear forces present across the L5-S1 IVD. The results of the current study are consistent with findings in clinical and biomechanical studies indicating that when SS and slip angle increase, patients may be predisposed to progression of lumbar spondylolisthesis and further disc degeneration at the lumbosacral level. 18,20,30 Furthermore, the increased vertical orientation of L5 may likely lead to anterior displacement.

Previous studies have discussed the relationship with the lumbar spine concerning SS changes, although to our knowledge, the current study is the first to quantify stresses on the hip joint and SIJ for changes in the SS. Our results regarding average hip joint contact stresses and maximum SIJ stresses are consistent with previous studies for the intact model and have been previously validated. ^{12,15,21,29} Even with the changes to the SS, stresses across

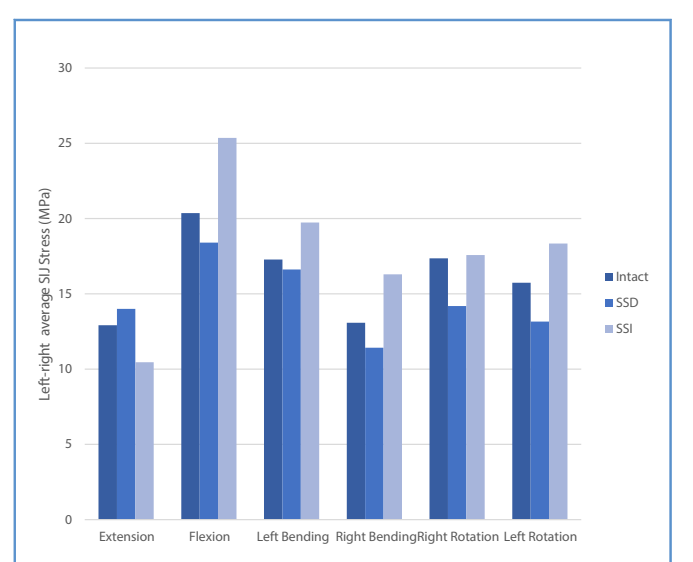


Figure 6. Left-right average sacroiliac joint contact stress for all motions. The *vertical axis* shows the stress (MPa) and the *horizontal axis* shows the motion. SSD, low sacral slope model: SSI, high sacral slope model.

the SIJ and hip joint showed reasonable differences with respect to these previously reported results. Results in the current study showed that the left-right average hip contact stress increased for most motions with a high SS angle, except for extension, which showed increased stress with a low SS angle. As SS increased, the lumbar spine and pelvis complex became more vertical, reducing the PT and maintaining a more vertical stance, which placed more load on the femoral heads. These results suggest that higher SS angles may increase stress on the femoral head. Many radiographic and FE studies have concluded that acetabular retroversion increases stresses on the acetabulum, which leads to osteoarthritis of the hip; however, to our knowledge, this study is the first to quantify results showing SS playing a role on the hip joint. 22,32,33 A study by Gebhart et al.34 examined 400 cadaveric skeletons and found a statistically significant correlation between increased PI and development of osteoarthritis in the hip, especially for younger individuals. The results in the present study agree with this study as PI is the algebraic sum of SS and PT. In a retrospective study examining hip joint narrowing after lumbar fusion, Kawai et al.35 reported that increased PI, SS, and LL all contributed to hip joint space narrowing after spinal fusion, further emphasizing that spinopelvic parameters play a role in development of increased stress on the hip joint.

Regarding the SIJ, few studies have examined SS and its relationship with SIJ dysfunction. A clinical study by Tonosu et al.^{36,37} examined how spinopelvic parameters were associated with SIJ pain. These investigators identified that patients with increased SS and LL experienced significantly higher pain scores in the SIJ pain group compared with the non-SIJ pain group. The results in the current study may numerically support this clinical finding because nearly all motions in the SSI group showed higher SIJ stresses, implying that SIJ dysfunction may be exacerbated in patients with a higher SS, although this requires further investigation. The case containing a low SS angle indicated lower SIJ stresses for all motions, except for extension, which showed higher stresses compared with both the intact model and SSI. In addition, both the patients with high SS and those with low SS for all motions resulted in the maximum SIJ stress being localized anteriorly (Figure 7).

The current FE study has some inherent limitations that need to be addressed. First, it lacks complex muscle forces, especially those of paraspinal muscles, which were replaced by follower loads and simplified muscles using elastic properties for the lower extremity. Second, this model did not consider age-related deformities as the mechanical behavior of the ligaments also changes with age.³⁸ In addition, producing different SS angles through the method described may differ compared with a study that uses patient-specific models. However, the angles mentioned earlier fell within the range of patients examined in a radiologic study by Os et al.2 and our models correspond to Type 1 (low SS and low PI) of Roussouly's 4 types. 17,39 It is necessary to verify whether lumbar slip is more likely to progress in types 2, 3 and 4 in the future. Conversely, adult spinal deformities, including lumbar kyphosis, should also be analyzed. 40 Future studies should examine several patient-specific models with varying SS angles to further understand mechanical changes at the hip joint and SIJ.

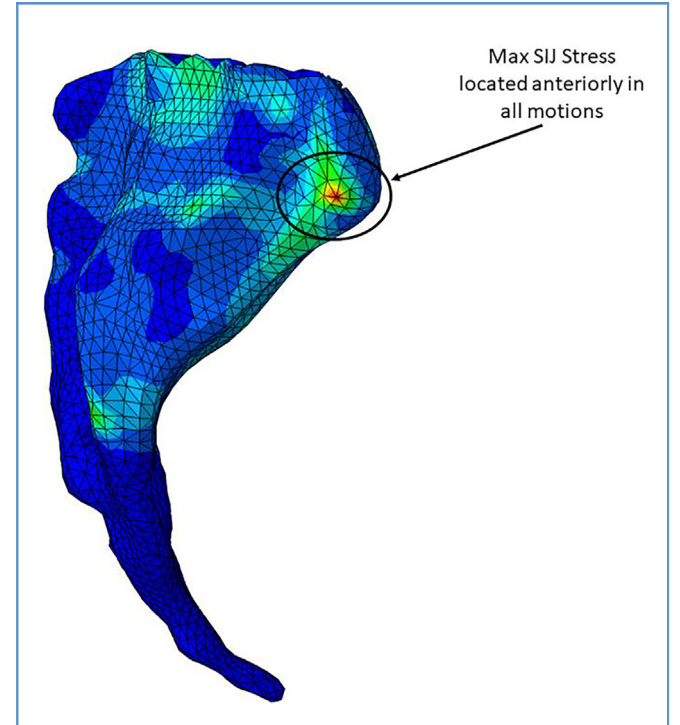


Figure 7. Maximum sacroiliac joint (Max SIJ) stress location, all motions showed a similar trend where the maximum stress was located anteriorly.

Degenerative changes such as lumbar alignment or femoral deformities were not examined, and future studies should examine how spinopelvic parameters influence diseases such as acetabular dysplasia. Despite these limitations, our biomechanical spine-pelvis-hip study provides valuable insights into different SS angles.

CONCLUSIONS

The present study indicated that the change in SS affects the biomechanical stress of the lumbar spine, SIJ, and hip joint. Correcting LL including SS is important but patients with high SS may have experience a negative impact on IVDs, SIJ, and hip joint. Clinicians should understand that a single parameter change can affect multiple joints and plan conservative or surgical treatments accordingly.

CREDIT AUTHORSHIP CONTRIBUTION STATEMENT

Yogesh Kumaran: Writing — original draft, Formal analysis, Data curation. Norihiro Nishida: Conceptualization, Methodology, Formal analysis, Data curation, Writing — original draft. Sudharshan Tripathi: Methodology, Formal analysis, Data curation. Muzammil Mumtaz: Methodology, Writing — review & editing. Takashi Sakai: Supervisor. Hossein Elgafy: Writing — review & editing. Vijay K. Goel: Supervisor.

REFERENCES

- I. Wang Z, Wang B, Yin B, Liu W, Yang F, Lv G. The relationship between spinopelvic parameters and clinical symptoms of severe isthmic spondylolisthesis: a prospective study of 64 patients. Eur Spine J. 2014;23:560-568.
- Oe S, Togawa D, Yoshida G, et al. Difference in spinal sagittal alignment and health-related quality of life between males and females with cervical deformity. Asian Spine J. 2017;11:959-967.
- Legaye J, Duval-Beaupère G, Hecquet J, Marty C. Pelvic incidence: a fundamental pelvic parameter for three-dimensional regulation of spinal sagittal curves. Eur Spine J. 1998;7:99-103.
- Hanke LF, Tuakli-Wosornu YA, Harrison JR, Moley PJ. The relationship between sacral slope and symptomatic isthmic spondylolysis in a cohort of high school athletes: a retrospective analysis. PM R. 2018;10:501-506.
- Mehta VA, Amin A, Omeis I, Gokaslan ZL, Gottfried ON. Implications of spinopelvic alignment for the spine surgeon. Neurosurgery. 2012;70:707-721.
- Labelle H, Mac-Thiong JM, Roussouly P. Spino-pelvic sagittal balance of spondylolisthesis: a review and classification. Eur Spine J. 2011;20(Suppl 5):641-646.
- Vialle R, Ilharreborde B, Dauzac C, Lenoir T, Rillardon L, Guigui P. Is there a sagittal imbalance of the spine in isthmic spondylolisthesis? A correlation study. Eur Spine J. 2007;16:1641-1649.
- Hanson DS, Bridwell KH, Rhee JM, Lenke LG. Correlation of pelvic incidence with low- and high-grade isthmic spondylolisthesis. Spine. 2002; 27:2026-2029.
- Roussouly P, Pinheiro-Franco JL. Biomechanical analysis of the spino-pelvic organization and adaptation in pathology. Eur Spine J. 2011;20(Suppl 5):609-618.
- 10. Jiang Y, Sun X, Peng X, Zhao J, Zhang K. Effect of sacral slope on the biomechanical behavior of the low lumbar spine. Exp Ther Med. 2017;13;2203-2210.
- II. Chen L, Feng Y, Che CQ, Gu Y, Wang LJ, Yang HL. Influence of sacral slope on the loading of pedicle screws in postoperative L5/S1 isthmic spondylolisthesis patient: a finite element analysis. Spine. 2016;41:E1388-E1393.
- Joukar A, Shah A, Kiapour A, et al. Sex specific sacroiliac joint biomechanics during standing Upright: afinite element study. Spine. 2018;43: E1053-E1060.
- Wu G, Siegler S, Allard P, et al. ISB recommendation on definitions of joint coordinate system of various joints for the reporting of human joint motion–part I: ankle, hip, and spine. International Society of Biomechanics. J Biomech. 2002;35:543-548.
- Anderson AE, Ellis BJ, Maas SA, Peters CL, Weiss JA. Validation of finite element predictions of cartilage contact pressure in the human hip joint. J Biomech Eng. 2008;130:051008.
- Harris MD, Anderson AE, Henak CR, Ellis BJ, Peters CL, Weiss JA. Finite element prediction of

- cartilage contact stresses in normal human hips. J Orthop Res. 2012;30:1133-1139.
- Bergmann G, Deuretzbacher G, Heller M, et al. Hip contact forces and gait patterns from routine activities. J Biomech. 2001;34:859-871.
- Roussouly P, Gollogly S, Berthonnaud E, Labelle H, Weidenbaum M. Sagittal alignment of the spine and pelvis in the presence of L5-s1 isthmic lysis and low-grade spondylolisthesis. Spine. 2006;31:2484-2490.
- Berlemann U, Jeszenszky DJ, Bühler DW, Harms J. The role of lumbar lordosis, vertebral end-plate inclination, disc height, and facet orientation in degenerative spondylolisthesis. J Spinal Disord. 1999;12:68-73.
- Phillips AT, Pankaj P, Howie CR, Usmani AS, Simpson AH. Finite element modelling of the pelvis: inclusion of muscular and ligamentous boundary conditions. Med Eng Phys. 2007;29:739-748.
- Funao H, Tsuji T, Hosogane N, et al. Comparative study of spinopelvic sagittal alignment between patients with and without degenerative spondylolisthesis. Eur Spine J. 2012;21:2181-2187.
- Bay BK, Hamel AJ, Olson SA, Sharkey NA. Statically equivalent load and support conditions produce different hip joint contact pressures and periacetabular strains. J Biomech. 1997;30:193-196.
- Hasegawa K, Kabata T, Kajino Y, Inoue D, Sakamoto J, Tsuchiya H. The influence of pelvic tilt on stress distribution in the acetabulum: finite element analysis. BMC Musculoskelet Disord. 2021;22: 764.
- Goel VK, Grauer JN, Patel T, et al. Effects of charité artificial disc on the implanted and adjacent spinal segments mechanics using a hybrid testing protocol. Spine. 2005;30:2755-2764.
- Dalstra M, Huiskes R, van Erning L. Development and validation of a three-dimensional finite element model of the pelvic bone. J Biomech Eng. 1995;117:272-278.
- Momeni Shahraki N, Fatemi A, Goel VK, Agarwal A. On the Use of Biaxial properties in modeling annulus as a Holzapfel-Gasser-Ogden material. Front Bioeng Biotechnol. 2015;3:69.
- Lindsey DP, Kiapour A, Yerby SA, Goel VK. Sacroiliac joint fusion Minimally affects adjacent lumbar Segment motion: afinite element study. Int J Spine Surg. 2015;9:64.
- Ivanov AA, Kiapour A, Ebraheim NA, Goel V. Lumbar fusion leads to increases in angular motion and stress across sacroiliac joint: a finite element study. Spine. 2009;34:E162-E169.
- Butler DL, Guan Y, Kay MD, Cummings JF, Feder SM, Levy MS. Location-dependent variations in the material properties of the anterior cruciate ligament. J Biomech. 1992;25:511-518.
- Joukar A, Chande RD, Carpenter RD, et al. Effects on hip stress following sacroiliac joint fixation: a finite element study. JOR Spine. 2019;2:e1067.

- 30. Drazin D, Hussain M, Harris J, et al. The role of sacral slope in lumbosacral fusion: a biomechanical study. J Neurosurg Spine. 2015;23:754-762.
- Oh YM, Choi HY, Eun JP. The Comparison of sagittal spinopelvic parameters between young adult patients with L5 spondylolysis and age-matched control group. J Korean Neurosurg Soc. 2013;54:207-210.
- 32. Kim WY, Hutchinson CE, Andrew JG, Allen PD. The relationship between acetabular retroversion and osteoarthritis of the hip. J Bone Joint Surg Br. 2006;88:727-729.
- **33.** Giori NJ, Trousdale RT. Acetabular retroversion is associated with osteoarthritis of the hip. Clin Orthop Relat Res. 2003:263-269.
- Gebhart JJ, Weinberg DS, Bohl MS, Liu RW. Relationship between pelvic incidence and osteoarthritis of the hip. Bone Joint Res. 2016;5:66-72.
- Kawai T, Shimizu T, Goto K, et al. The impact of spinopelvic parameters on hip degeneration after spinal fusion. Spine (Phila Pa 1976). 2022;47:1093-1102.
- Tonosu J, Oka H, Watanabe K, et al. Characteristics of the spinopelvic parameters of patients with sacroiliac joint pain. Sci Rep. 2021;11:5189.
- Tonosu J, Kurosawa D, Nishi T, et al. The association between sacroiliac joint-related pain following lumbar spine surgery and spinopelvic parameters: a prospective multicenter study. Eur Spine J. 2014;28:1603-1609.
- 38. Mihara A, Nishida N, Jiang F, et al. Tensile test of human lumbar ligamentum flavum: age-related changes of stiffness. Appl Sci. 2021;11:3337.
- Mac-Thiong J-M, Labelle H. A proposal for a surgical classification of pediatric lumbosacral spondylolisthesis based on current literature. Eur Spine J. 2006;15:1425-1435.
- 40. Roussouly P, Gollogly S, Berthonnaud E, Dimnet J. Classification of the normal variation in the sagittal alignment of the human lumbar spine and pelvis in the standing position. Spine. 2005;30:346-353.

Conflict of interest statement: The work was supported in part by the NSF Industry/University Cooperative Research Center at University of California San Francisco, San Francisco, California; Ohio State University, Columbus, Ohio; University of Toledo, Toledo, Ohio (www.nsfcdmi.org); and the AO Foundation.

Received 22 January 2023; accepted 14 March 2023 Citation: World Neurosurg. (2023) 176:e32-e39.

Journal homepage: www.journals.elsevier.com/world-neurosurgery

Available online: www.sciencedirect.com

https://doi.org/10.1016/j.wneu.2023.03.057

1878-8750/\$ - see front matter © 2023 Elsevier Inc. All rights reserved.